Density Functional Theory Investigation of Hydrogen Bonding Effects on the Oxygen, Nitrogen and Hydrogen Electric Field Gradient and Chemical Shielding Tensors of Anhydrous Chitosan Crystalline Structure

Mehdi D. Esrafili, Fatemeh Elmi, and Nasser L. Hadipour*

Department of Chemistry, Tarbiat Modares University, P.O. Box 14115-175, Tehran, Iran

Received: October 14, 2006; In Final Form: December 5, 2006

A systematic computational investigation was carried out to characterize the ^{17}O, ^{14}N and ^{2}H electric field gradient, EFG, as well as ^{17}O, ^{15}N, ^{13}C and ^{1}H chemical shielding tensors in the anhydrous chitosan crystalline structure. To include the hydrogen-bonding effects in the calculations, the most probable interacting molecules with the target molecule in the crystalline phase were considered through a hexameric cluster. The computations were performed with the B3LYP method and 6-311++G(d,p) and 6-31++G(d,p) standard basis sets using the Gaussian 98 suite of programs. Calculated EFG and chemical shielding tensors were used to evaluate the ^{17}O, ^{14}N and ^{2}H nuclear quadrupole resonance, NQR, and ^{17}O, ^{15}N, ^{13}C and ^{1}H nuclear magnetic resonance, NMR, parameters in the hexameric cluster, which are in good agreement with the available experimental data. The difference between the calculated NQR and NMR parameters of the monomer and hexamer cluster shows how much hydrogen bonding interactions affect the EFG and chemical shielding tensors of each nucleus. These results indicate that both O(3)−H(33)···O(5−3) and N−H(22)···O(6−4) hydrogen bonding have a major influence on NQR and NMR parameters. Also, the quantum chemical calculations indicate that the intra- and intermolecular hydrogen bonding interactions play an essential role in determining the relative orientation of EFG and chemical shielding principal components in the molecular frame axes.

1. Introduction

Hydrogen bonds, HBs, play an essential role in natural phenomena, especially in the chemical and biochemical systems. Stabilization of polysaccharide chains, for example, is due to the formation of a network of intra- and intermolecular HBs. In many cases, the type of these HBs is O−H···O and N−H···O, which, like any other hydrogen bond, are electrostatic in nature.[1]

It is an interesting subject to investigate the effects of long-range interactions such as hydrogen bonding, H-bonding, in chitosan and its derivatives because of their key roles such as drug delivery, antitumor and cholesterol lowering materials in biosystems.[2−6] Moreover, understanding the nature of these interactions can be crucial in describing the function of these systems in biological media at the molecular level. Numerous investigations in various experimental and theoretical fields have been done to characterize these H-bonding interactions in both solid and liquid states on anhydrous polymorph of chitosan and its derivatives[7−10]

Solid-state nuclear magnetic resonance, NMR, spectroscopy including both static and magic angle spinning, MAS, techniques seems to be an efficient approach to study the nature of intra- and intermolecular H-bonding interactions in the crystalline phase.[11−15] Recently, CP/MAS NMR studies have been reported for both magnetically active ^{13}C and ^{15}N nuclei in chitosan anhydrous polymorph.[16,17] The chemical shielding interaction of the nuclear magnetic moment with the magnetic field induced by the surrounding electron density is represented by the chemical shielding tensor.[18] More specifically, information regarding the chemical shielding isotropy and anisotropy parameters include valuable insights on the local bonding environment and electronic structure of the molecule in its crystalline phase.[19−22] In addition, systematic analysis of the symmetric part of the chemical shielding tensor yields worthwhile information about the magnitude and orientation of its principal components in the molecular frame axes, which are directly related to the nature of NMR interactions.[18,23−25]

In congruence with the nuclear magnetic approach, the study of the nuclear electric quadrupole interaction with the originated electric field gradient, EFG, at the quadrupole nuclei, is often used as another powerful tool to investigate the H-bonding effects in the crystalline phase.[26−28] Experimentally, such interactions are studied well with nuclear quadrupole resonance, NQR, spectroscopy. The electric quadrupole moment, eQ, is a characteristic of a nucleus with spin angular momentum, I, greater than one-half, $I > {}^1/_2$, which is a measure of the nuclear charge distortion from the spherical shape.[29] In fact, the quadrupole coupling constant, C_Q, and asymmetry parameter, η_Q, are experimentally measurable NQR parameters of which the former indicates the interaction of EFG and eQ whereas the latter measures the amount of symmetry of EFG tensor.[30] Although, NQR parameters can be theoretically obtained, no experimental study for anhydrous chitosan has yet been carried out.

The assumption is that high level quantum mechanical methods are often used to evaluate EFG and chemical shielding tensors. This may be done for oxygen, nitrogen, hydrogen and carbon atoms of anhydrous chitosan in its crystalline phase. Although the experimental studies are essential in obtaining information about the HBs, combining them with theoretical calculations leads to better interpretation of experimental NQR and NMR parameters and can be used for structural analysis.

* Corresponding author. E-mail: hadipour@modares.ac.ir.

10.1021/jp066761r CCC: $37.00
Published on Web 01/13/2007

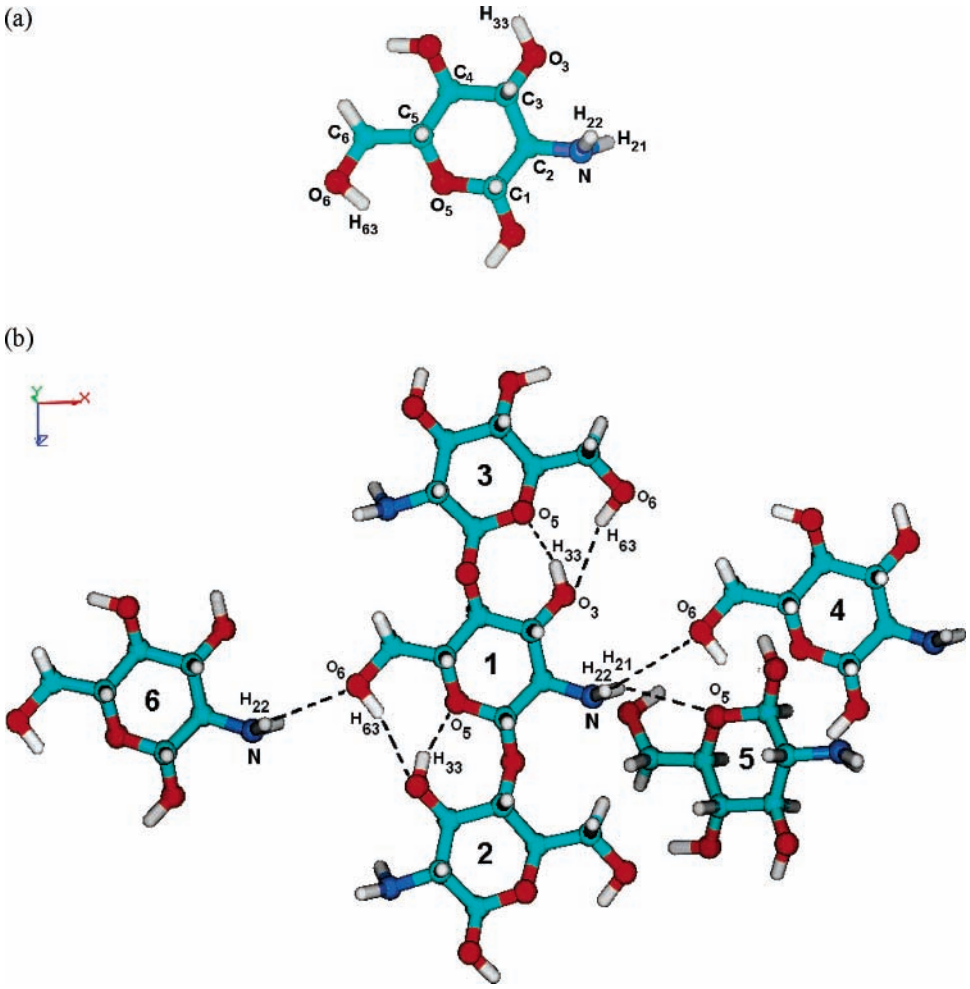

Figure 1. (a) Monomer and (b) intra- and intermolecular H-bonding interactions in the hexameric cluster of anhydrous chitosan

To the best of our knowledge, in spite of the fact that experimental ^{15}N chemical shielding isotropy studies were performed on anhydrous chitosan,[17,31] there is still a lack of systematic computational investigation about the magnitude and relative orientation of the nitrogen chemical shielding tensor in the literature.

It is well recognized that determining the strength and geometry of HBs is a challenge for both experimental and theoretical studies. Regarding theoretical works, ab initio methods accounting for electron correlation are needed for an accurate description of HBs. Therefore, Hartree−Fock calculations are not applicable to such situations. Also large enough basis sets are necessary to expand the wave function.[32] Thus, to make an accurate description of hydrogen-bonded system with ab initio correlated methods together with high quality basis sets is really demanding. Density functional theory, DFT, is widely used in computational chemistry due to its excellent performance-to-cost ratio. There are many flavors of approximations to $E_{XC}[\rho]$ in use today. Various studies reveal that the generalized gradient approximations (GGA) and hybrid functional are more accurate than local-density approximations (LDA) to describe the HBs.[32−36]

DFT is currently the most popular electronic structure method. In spite of the known deficiency of DFT to describe the dispersion energy, it offers many advantages. The long-range dispersion interaction between two molecules cannot be described well with the standard used approximate density functionals. However, the dispersion coefficients that describe the interactions can be calculated well with DFT response calculations.[37] In this paper, we focused on properties that require information of one electronic state at a single point on the potential energy surface which are the electric field gradient and nuclear magnetic shielding as first and second-order properties, respectively. Various DFT studies of electric,[38] magnetic,[39] and electromagnetic[40−42] linear response properties indicate that the B3LYP functional performs better than BLYP functional.

Previous studies demonstrate the reproduction quality and reliability of calculated NQR and NMR parameters obtained from real crystalline structures.[43−45] In this research, anhydrous polymorph of chitosan is regarded as a hexameric cluster where the most probable interacting polymeric chains with the target molecule are considered as chitosan monomeric units. As Figure 1 illustrates, target molecule interacts directly with the five nearest neighbors through the intra- and intermolecular HBs. Because of the essential role of these H-bonding interactions in the stabilization and giving the 3-D structure to chitosan chains, our main objective is to study the effects of these HBs on the calculated EFG and chemical shielding tensors. The calculated NQR parameters from the diagonal components of EFG tensors, C_Q and η_Q, are shown in Tables 2−4. The calculated chemical shielding tensors were used to evaluate the chemical shielding isotropy and anisotropy values for ^1H, ^{15}N and ^{17}O in their principal axes system, PAS, which are summarized and represented in Tables 5 and 6. Finally, the relative orientation of the EFG and chemical shielding tensors of the oxygen and nitrogen atoms in the molecular frame are obtained and tabulated in Table 7.

TABLE 1: Distance (Å) between Interactive Atoms of Anhydrous Chitosan in the Cluster

r[target...neighbor][a,b]	distance (Å)
r[O(3)···H(63) − 3:0.5 − *x*, − *y*, *z* + 0.5]	2.268
r[H(63)···O(3) − 2:0.5 − *x*, − *y*, *z* − 0.5]	2.268
r[O(6)···H(22) − 6:1 − *x*, *y*, *z*]	1.602
r[H(21)···O(5) − 5:0.5 + *x*, − 1 − *y*, 1 − *z*]	2.518
r[H(22)···O(3) − 4:1 + *x*, *y*, *z*]	1.602
r[O(5)···H(33) − 2:0.5 − *x*, − *y*, *z* − 0.5]	1.671
r[H(33)···O(5) − 3:0.5 − *x*, − *y*, *z* + 0.5]	1.671

[a] The number in parentheses denotes the atom number and the second one denotes the molecule number as indicated in Figure 1. [b] Hydrogen atom positions are optimized by the B3LYP/6-31++G(d,p) method.

TABLE 2: Calculated[a] EFG Tensors of ^{17}O and ^{14}N

		q_{ii}[b]		C_Q[c]		η_Q	
nucleus	q_{ii}	monomer	cluster	monomer	cluster	monomer	cluster
O(3)	q_{xx}	−0.183	−0.033				
		(−0.183)	(−0.040)				
	q_{yy}	−1.771	−1.718	11.75	10.52	0.81	0.97
		(−1.62)	(−1.543)	(10.84)	(9.52)	(0.78)	(0.95)
	q_{zz}	1.955	1.751				
		(1.803)	(1.583)				
O(5)	q_{xx}	−0.371	−0.438				
		(−0.089)	(−0.138)				
	q_{yy}	−1.805	−1.738	11.41	11.33	0.90	0.85
		(−1.636)	(−1.554)	(10.37)	(10.16)	(0.89)	(0.84)
	q_{zz}	1.898	1.884				
		(1.724)	(1.692)				
O(6)	q_{xx}	−0.371	−0.438				
		(−0.362)	(−0.405)				
	q_{yy}	−1.709	−1.603	12.51	12.27	0.64	0.57
		(−1.554)	(−1.453)	(11.52)	(11.17)	(0.62)	(0.56)
	q_{zz}	2.080	2.041				
		(1.916)	(1.859)				
N	q_{xx}	−0.548	−0.829				
		(−0.709)	(−0.801)				
	q_{yy}	−0.789	−0.361	6.42	5.71	0.30	0.39
		(−0.514)	(−0.358)	(5.88)	(5.57)	(0.27)	(0.38)
	q_{zz}	1.337	1.189				
		(1.233)	(1.159)				

[a] Results obtained by B3LYP/6-311++G(d,p). Results in parentheses obtained by B3LYP/6-31++G(d,p). [b] q_{ii} values in atomic units, 1 au = 9.717365 × 10^{21} V m^{-2}. [c] Calculated C_Q values in MHz.

2. Theory

Chemical shielding Hamiltonian acting on a spin, *I*, is given by[46]

$$\hat{H} = -\gamma\hbar\sigma B_0\hat{I} \tag{1}$$

where γ, B_0 and $\hat{I}$ are magnetogyric ratio, applied magnetic field and nuclear spin operator, respectively. The term σ is a second-rank tensor called the NMR chemical shielding tensor whose elements describe the size of chemical shielding as a function of molecular orientation respecting to the external magnetic field. In PAS, this tensor is converted to a diagonal matrix with σ_{11}, σ_{22} and σ_{33} components where $\sigma_{33} > \sigma_{22} > \sigma_{11}$. To describe a chemical shielding tensor, chemical shielding isotropy, σ_{iso}, and anisotropy, $\Delta\sigma$, are used in addition to the three principal components. These two NMR parameters are related to the principal components by following equations:

$$\sigma_{iso} = \frac{1}{3}(\sigma_{11} + \sigma_{22} + \sigma_{33}) \tag{2}$$

$$\Delta\sigma = \sigma_{33} - \frac{1}{2}(\sigma_{11} + \sigma_{22}) \tag{3}$$

TABLE 3: Calculated[a] EFG Tensors of ^{2}H

		q_{ii}[b]		C_Q[c]		η_Q	
nucleus	q_{ii}	monomer	cluster	monomer	cluster	monomer	cluster
H(21)	q_{xx}	0.147	0.148				
		(0.139)	(−0.140)				
	q_{yy}	0.234	0.225	256.40	250.93	0.23	0.21
		(0.227)	(0.218)	(246.26)	(240.96)	(0.24)	(0.22)
	q_{zz}	−0.381	−0.373				
		(−0.366)	(−0.358)				
H(22)	q_{xx}	0.151	0.1340				
		(0.143)	(0.127)				
	q_{yy}	0.234	0.200	258.36	224.72	0.22	0.20
		(0.227)	(0.194)	(248.25)	(216.20)	(0.23)	(0.21)
	q_{zz}	−0.384	−0.334				
		(−0.369)	(−0.322)				
H(33)	q_{xx}	0.157	0.116				
		(0.151)	(0.109)				
	q_{yy}	0.216	0.199	250.31	212.31	0.16	0.26
		(0.211)	(0.194)	(243.00)	(204.08)	(0.17)	(0.28)
	q_{zz}	−0.372	−0.316				
		(−0.362)	(−0.304)				
H(63)	q_{xx}	0.136	0.139				
		(0.129)	(0.134)				
	q_{yy}	0.207	0.200	230.53	228.51	0.21	0.18
		(0.203)	(0.197)	(222.86)	(223.08)	(0.22)	(0.19)
	q_{zz}	−0.343	−0.339				
		(−0.332)	(−0.332)				

[a] Results obtained by B3LYP/6-311++G(d,p). Results in parentheses obtained by B3LYP/6-31++G(d,p). [b] q_{ii} values in atomic units, 1 au = 9.717365 × 10^{21} V m^{-2}. [c] Calculated C_Q values in kHz.

TABLE 4: BSSE of NQR Parameters[a] (q_{ii}, C_Q (MHz) and η_Q) of Anhydrous Chitosan

nucleus	Δq_{xx}[b]	Δq_{yy}[b]	Δq_{zz}[b]	ΔC_Q	$\Delta\eta_Q$
O(3)	0.004	0.002	0.001	0.006	0.002
	(0.008)	(0.004)	(0.002)	(0.012)	(0.006)
O(5)	0.003	0.001	0.002	0.003	0.005
	(0.008)	(0.005)	(0.007)	(0.013)	(0.014)
O(6)	0.0020	0.003	0.001	0.006	0.005
	(0.004)	(0.007)	(0.002)	(0.012)	(0.008)
N	0.001	0.001	0.003	0.014	0.003
	(0.003)	(0.004)	(0.005)	(0.024)	(0.002)
H(21)	0.000	0.001	0.000	0.000	0.000
	(0.001)	(0.001)	(0.000)	(0.000)	(0.001)
H(22)	0.001	0.002	0.001	0.000	0.001
	(0.002)	(0.003)	(0.002)	(0.001)	(0.003)
H(33)	0.001	0.000	0.000	0.000	0.000
	(0.002)	(0.001)	(0.002)	(0.001)	(0.001)
H(63)	0.000	0.001	0.000	0.000	0.000
	(0.000)	(0.002)	(0.000)	(0.000)	(0.001)

[a] Results obtained by B3LYP/6-311++G(d,p). Results in parentheses obtained by B3LYP/6-31++G(d,p). [b] Calculated Δq_{ii} values in au.

The interaction between nuclear electric quadrupole moment and EFG at quadrupole nucleus is described with Hamiltonian as follows:

$$\hat{H} = \frac{e^2Qq_{zz}}{4I(2I-1)}[(3\hat{I}_z^2 - \hat{I}^2) + \eta_Q(\hat{I}_x^2 - I_y^2)] \tag{4}$$

where eQ is the nuclear electric quadrupole moment, I is the nuclear spin, and q_{zz} is the largest component of the EFG tensor. The principal components of the EFG tensor, q_{ii}, are computed in atomic units (1 au = 9.717365 × 10^{21} V m^{-2}), with $|q_{zz}| \geq |q_{yy}| \geq |q_{xx}|$ and $q_{xx} + q_{yy} + q_{zz} = 0$. These diagonal elements relate to each other by the asymmetry parameter: $\eta_Q = (|q_{yy} - q_{xx}|)/|q_{zz}|$, $0 \leq \eta_Q \leq 1$, which measures the deviation of EFG tensor from axial symmetry. The computed q_{zz} component of EFG tensor is used to obtain the nuclear quadrupole coupling constant from the equation; $C_Q = e^2Qq_{zz}/h$.[47]

TABLE 5: Calculated[a] Chemical Shielding Tensors of ^{17}O and ^{15}N

		σ_{ii}[b]		σ_{iso}		$\Delta\sigma$	
nucleus	σ_{ii}	monomer	cluster	monomer	cluster	monomer	cluster
O(3)	σ_{11}	231.06	235.11				
		(247.69)	(248.67)				
	σ_{22}	256.66	255.27	266.90	259.59	55.899	43.23
		(277.69)	(269.01)	(279.53)	(273.11)	(50.54)	(42.84)
	σ_{33}	304.25	288.41				
		(313.22)	(301.67)				
O(5)	σ_{11}	160.75	171.27				
		(179.83)	(188.27)				
	σ_{22}	227.02	220.16	213.66	215.34	59.33	58.80
		(240.51)	(232.74)	(229.02)	(228.66)	(56.57)	(54.48)
	σ_{33}	253.22	254.59				
		(266.74)	(264.99)				
O(6)	σ_{11}	241.56	230.38				
		(256.18)	(244.09)				
	σ_{22}	286.05	257.74	298.97	280.18	105.48	108.61
		(299.04)	(268.52)	(309.38)	(289.85)	(95.29)	(100.64)
	σ_{33}	369.29	352.59				
		(372.90)	(356.95)				
N	σ_{11}	174.03	179.47				
		(184.66)	(179.99)				
	σ_{22}	231.25	224.17	222.32	220.79	59.03	56.94
		(238.82)	(229.23)	(230.24)	(223.62)	(54.91)	(57.03)
	σ_{33}	261.67	258.73				
		(261.67)	(261.64)				

[a] Results obtained by B3LYP/6-311++G(d,p). Results in parentheses obtained by B3LYP/6-31++G(d,p). [b] Calculated σ_{ii}, σ_{iso} and $\Delta\sigma$ values in ppm.

TABLE 6: Calculated[a] Chemical Shielding Tensors of ^{1}H

		σ_{ii}[b]		σ_{iso}		$\Delta\sigma$	
nucleus	σ_{ii}	monomer	cluster	monomer	cluster	monomer	cluster
H(21)	σ_{11}	23.59	22.08				
		(23.16)	(21.99)				
	σ_{22}	26.27	25.90	29.82	29.63	14.67	16.93
		(25.76)	(25.74)	(29.49)	(29.55)	(15.10)	(17.04)
	σ_{33}	29.60	40.92				
		(39.56)	(40.91)				
H(22)	σ_{11}	25.57	11.92				
		(25.15)	(11.72)				
	σ_{22}	28.35	15.46	31.51	24.85	13.64	33.47
		(27.96)	(15.60)	(31.21)	(24.83)	(13.96)	(33.52)
	σ_{33}	40.61	47.17				
		(40.52)	(47.18)				
H(33)	σ_{11}	19.57	8.48				
		(18.97)	(8.04)				
	σ_{22}	28.07	20.09	29.04	25.29	15.66	33.00
		(27.63)	(20.00)	(28.63)	(25.13)	(15.97)	(33.32)
	σ_{33}	39.48	47.30				
		(39.27)	(47.35)				
H(63)	σ_{11}	19.80	19.78				
		(19.35)	(16.52)				
	σ_{22}	32.07	29.23	30.13	28.52	12.57	16.75
		(31.47)	(28.32)	(29.74)	(29.06)	(13.00)	(19.94)
	σ_{33}	38.50	42.41				
		(38.40)	(42.36)				

[a] Results obtained by B3LYP/6-311++G(d,p). Results in parentheses obtained by B3LYP/6-31++G(d,p). [b] Calculated σ_{ii}, σ_{iso} and $\Delta\sigma$ values in ppm.

3. Computational Aspects

DFT calculations were performed using the Gaussian 98 suite of programs.[48] This is done for calculating the EFG and chemical shielding tensors in their PAS for oxygen, nitrogen, carbon and hydrogen atoms. Among various modern functionals for DFT calculation, Becke's three parameter hybrid functional combined with the Lee−Yang−Parr correlation functional, designated B3LYP, with 6-311++G(d,p) and 6-31++G(d,p) standard basis sets were used.[49] Various combinations of diffuse and polarization functions are incorporated in these two basis sets that are necessary for computation of EFG and chemical shielding tensors of hydrogen, nitrogen and oxygen atoms involved in HBs. Our pervious experiences reveal that 6-311++G(d,p) and 6-31++G(d,p) usually lead to satisfactory EFG and chemical shielding values.[43,44,50] Recent studies suggest that the B3LYP level of theory using the 6-311++G(d,p) basis set can yield adequate accurate results to calculate ^{14}N,^{17}O chemical shielding and electric field gradient.[22,44,50,51]

TABLE 7: Calculated (B3LYP/6-311++G(d,p)) Euler Angles (deg) of Oxygen and Nitrogen Atoms of the Target Molecule in the Hexameric Cluster

nucleus	α	β	γ
O(3)	67.15	91.87	109.19
O(5)	81.12	142.37	96.92
O(6)	67.78	106.95	74.00
N	78.49	122.03	88.41

The crystal structure of anhydrous chitosan from X-ray diffraction study[52] was used to evaluate EFG and chemical shielding parameters based on DFT calculations. For both single and cluster molecules, the atomic coordinates extracted from X-ray diffractions. Because of the deficiency of X-ray diffraction to locate the accurate position of hydrogen atoms, the optimization of hydrogen atoms coordinates was needed. The B3LYP/6-31++G(d,p) level of theory was performed to optimize only the hydrogen atoms position while other atoms position were held fixed. Figure 1 shows the central molecule, molecule number 1, is surrounded with five other molecules which participate in intra- and intermolecular H-bonding interactions with central molecule. EFG and chemical shielding parameters were calculated for central molecule. The results confirm that the EFG and chemical shielding tensors are sensitive to the formation of intra- and intermolecular HBs.

Chemical shielding calculations were performed using the gauge included atomic orbital, GIAO, method.[53] Because quantum chemical calculations yield absolute chemical shielding values, one must establish the absolute shielding value for a particular nucleus to obtain a direct relation between the calculated results and experimentally reported data. To evaluate the chemical shift isotropy of carbons and nitrogen, δ_{iso}, from the calculated $\sigma_{iso,cal}$ values, we used

$$\delta_{iso} = \sigma_{iso,ref} - \sigma_{iso,cal} \quad (5)$$

where $\sigma_{iso,ref}$ refers to the absolute chemical shielding isotropy of tetramethylsilane (TMS) and ammonium nitrate (phase IV) with $\sigma_{iso,ref} = 184.1$ and 223.4 ppm, respectively.[54,55]

The nuclear electric quadrupole moment values of ^{2}H, ^{14}N and ^{17}O have been reported by Pyykkö as 2.86, 20.44 and −25.58 mb, respectively.[56]

4. Results and Discussion

In this work, we attempted to investigate the ^{17}O, ^{14}N and ^{2}H EFG tensors as well as ^{17}O, ^{15}N, ^{1}H and ^{13}C chemical shielding tensors of the anhydrous polymorph of chitosan in the solid phase. Because the cluster model of anhydrous chitosan was considered, it was expected that the calculated results would be close to those quantities that measured by the experimental devices. The results are summarized in Tables 2−6.

Figure 1, which is constructed using X-ray diffraction atomic coordinates, shows that chitosan makes a variety of intra- and

intermolecular HBs in the solid phase. Considering this fact, a hexameric cluster was created. Hydrogen bond distances were summarized and represented in Table 1. To demonstrate the importance of H-bonding interactions, two sets of calculations were performed. First, we calculated EFG and chemical shielding tensors for isolated molecule (monomer) and then we did the same for target molecule and finally we compared the calculations for the monomer and target molecule. In the following section, we will discuss the EFG, chemical shielding tensor calculations and orientation of their principal components in the molecular frame axes, separately.

4.1. Electric Field Gradient Tensors. In this part, the DFT calculations at the B3LYP level of theory with the 6-311++G(d,p) and 6-31++G(d,p) basis sets were carried out to study the H-bonding effects on the ^{17}O, ^{14}N and ^{2}H EFG tensors of anhydrous chitosan. The calculated EFG tensor principal components, nuclear quadrupole coupling constants, C_Q, and asymmetry parameters, η_Q, for ^{17}O, ^{14}N and ^{2}H are summarized in Tables 2−4.

At first glance at the calculated results, some interesting trends can be easily obtained. First, for those nuclei participated in the H-bonding interactions, the EFG tensor exhibits significantly changes on going from the isolated molecule model to the target molecule in the cluster. On the other hand, the C_Q values of those nuclei that contribute in the H-bonding interactions decrease, but their η_Q values do not indicate a regular pattern from the isolated gas phase to the cluster. Of course, the magnitude of these changes at each nucleus depends directly on its amount of contribution to the interactions. Second, considering the calculated EFG tensors by 6-311++G(d,p) and 6-31++G(d,p), it is clear that the results obtained by these basis sets are practically coincident with each other. The results of 6-311++G(d,p) are reported in the paper.

As the results in Tables 2 and 3 indicate, H-bonding interactions have different influences on the calculated ^{17}O, ^{14}N and ^{2}H nuclei. O(3) with noticeable $\Delta C_Q(^{17}O) = 1.23$ MHz and $\Delta\eta_Q = 0.16$ is the most affected nucleus of the target molecule in the H-bonding interactions. More specifically, for this nucleus the change in the largest component of the EFG tensor, q_{zz}, is more pronounced than q_{xx} and q_{yy} through the formation of H-bonding interactions. These effects suggest that the intramolecular hydrogen bond interactions at the O(3) in crystalline anhydrous chitosan is rather strong. On the other hand, because H(33) and H(22) atoms have proper distances to formation HBs, r[H(33)···O(5)-3] = 1.671 Å and r[H(22)···O(6)-4] = 1.602 Å, they have major changes in the EFG tensor among the hydrogen atoms; see Table 3. For these nuclei, $\Delta C_Q(^{2}H) = 38.0$ and 33.64 kHz and $\Delta\eta_Q = 0.10$ and 0.02 values reveal the greater importance of the O(3)−H(33) and NH_2 functional groups in contributing to the strong HBs in the crystalline anhydrous chitosan.

For the EFG tensor at the O(6) site, the comparison of the isolated model and the hexameric cluster shows some discrepancy, although not as dramatic as the one seen for O(3). By a quick look at Figure 1, it is found that the O(6) atom of the target molecule also can form an intermolecular hydrogen bond with molecule number 6, which is located at an adjacent parallel chain. From having two possibilities to formation of HBs, r[O(6)−H(63)···O(3−2)] = 2.268 Å and r[O(6)···H(22−6)] = 1.602 Å, $C_Q(^{17}O)$ and η_Q for O(6) decrease by 0.24 MHz and 0.07 from the monomer to the target molecule in the cluster, respectively. On the other hand, in contrast to O(3) and O(6), the EFG tensor of O(5) shows less sensitivity to H-bonding interactions. Having the proper hydrogen bond distance, r[O(5)···H(33−2)] = 1.671 Å, the $C_Q(^{17}O)$ value decreases by only 0.08 MHz and η_Q by 0.05, as a consequence of involving in the intramolecular H-bonding interactions.

As Figure 1 indicates, the HBs at the NH_2 site of the target molecule involve O(6−4) and O(5−5) atoms of two neighboring molecules. X-ray crystallography data reveal that in the crystalline phase, the anhydrous chitosan chain has both parallel and antiparallel sheet structure with respect to neighboring chains.[52] By a quick look at the entire unit cell, it is obvious that one of these H-bonding interactions joins polymeric chains in the same layer (molecules 1 and 4), whereas the other hydrogen bond is formed by interaction between the molecules of two antiparallel chains. As mentioned above, the N−H(22)···O(6) hydrogen bond has a significant effect on the $^{17}O(6)$ EFG tensor. As Table 2 indicates, from the monomer to the target molecule in the cluster, H-bonding interactions cause a 0.71 MHz reduction in the $C_Q(^{14}N)$ parameter. It is also interesting to see that the η_Q value for this nucleus increases 0.09 units depending on whether the chitosan is in the monomer or in the H-bonding network. These features reveal the major role of the NH_2 group in contributing to the intermolecular H-bonding interactions in the crystalline anhydrous chitosan.

Finally, the basis set superposition error, BSSE,[57] was determined for the magnitude of principal components of ^{17}O, ^{14}N and ^{2}H EFG tensors of anhydrous chitosan. It might also be mentioned that EFG and chemical shielding counterpoise corrections were also reported elsewhere.[58−63] Chesnut and Rusilowski concluded on the basis of calculation of the chemical shieldings of $(H_2O)_2$ and $(HF)_2$ dimers that for the heavy atoms employing diffuse functions in the basis set can remove the need for their counterpoise corrections.[61]

As can be seen from Table 3, it was found that BSSE for the 6-311++G(d,p) basis set is less than 0.01 au in the principal components of all oxygen, nitrogen and hydrogen atoms. Although the basis set dependence affects slightly the calculated EFG tensors, these changes are an order of magnitude smaller than the changes observed between the calculations on the chitosan cluster and isolated molecule. The largest BSSE for the principal components of the EFG tensor at the nitrogen position was found to be 0.003 au at the q_{zz} where the other two principal components were within 0.001 au. Hence EFG tensor calculations were not counterpoise corrected, and none of these problems affects the validity of the results discussed above.

4.2. Chemical Shielding Tensors. As the general trend was shown in the previous section, the EFG tensors at the ^{17}O, ^{14}N and ^{2}H nuclei have significant sensitivity on the intra- and intermolecular HBs formation. In this part, we will focus on the effects of H-bonding interactions on the ^{17}O, ^{15}N, ^{13}C and ^{1}H chemical shielding tenors. To achieve the aim, B3LYP/6-311++G(d,p) and B3LYP/6-31++G(d,p) calculations were carried out for both forms of isolated gas phase and hexameric cluster of anhydrous chitosan. As mentioned above, both structures were taken from X-ray crystallography data. The calculated chemical shielding tensors were reported as chemical shielding principal components, σ_{ii}, chemical shielding isotropy, σ_{iso}, and chemical shielding anisotropy, $\Delta\sigma$, in Tables 5 and 6.

As the results in Tables 5 and 6 indicate, the calculated chemical shielding tensors show some trends parallel with those discussed in the EFG tensor for various nuclei of anhydrous chitosan. B3LYP/6-311++G(d,p) calculation reveals that due to the H-bonding interactions, the nitrogen of the $-NH_2$ group is deshielded 1.53 ppm in σ_{iso} and 2.12 ppm in $\Delta\sigma$ values from the isolated monomer to the target molecule in the cluster. The

calculated σ_{iso} value for ^{15}N of the target molecule has been obtained to be 220.70 ppm. This value, which is obtained by taking the whole cluster into consideration, is expected to be close to the experimental value. However, the experimental ^{15}N chemical shielding of chitosan has been found to be 213.4 ppm,[17] so our calculated σ_{iso} value deviates by 3.46% from the experimental value. This result illustrates that the NH_2 site of the target molecule approximately feels the same chemical environment as in the actual solid phase. The remaining discrepancy between the calculated and observed ^{15}N isotropic parameter is believed to be led partly from the used simplified molecular model. Moreover, a portion of this discrepancy between the theoretical and calculated ^{15}N chemical shielding value can be attributed to the intrinsic limitation of the present theoretical calculations.

In agreement with the EFG tensor calculations, the changes in ^{17}O shielding values are also significant. As Table 5 shows, the calculated chemical shielding tensors of the O(5) atom are more affected by H-bonding formation than the EFG tensors. Due to the inclusion of H-bonding interactions, changes in the ^{17}O chemical shielding isotropy and anisotropy of O(3) nucleus are also accompanied by a reduction of approximately 7 and 12 ppm, respectively. It interacts with both O(5−3) and O(6−3) atoms of the molecule number 2 along the polymeric chain. Because of the different natures of the O(3) atom in intramolecular H-bonding interactions (proton donor and proton acceptor) and different chemical environments, the NMR parameters change more than those for O(5). Furthermore, because the capability of O(6) in the formation of two HBs, the changes in its chemical shielding tensor are significant. From the monomer to the target molecule in the cluster, σ_{iso} and $\Delta\sigma$ values decrease approximately 18 and 3 ppm for O(6), respectively, indicating the importance of O(6) atom in contributing to the HBs in the crystalline anhydrous chitosan.

The obtained chemical shielding results for H(33) and H(22) also have the remarkable changes among the ^1H nuclei of anhydrous chitosan. Because both nuclei participate in strong HBs, σ_{iso} values decrease approximately 4 and 7 ppm from the monomer to the cluster, respectively. On the other hand, the changes in the NMR parameters of H(21) are not noticeable from the monomer to the cluster; see Table 6. This is due to the limited involvement of this nucleus in weak H(21)···O(5−5) H-bonding interaction, r[H(21)···O(5−5)] = 2.518 Å. Except for the σ_{33} component of calculated chemical shielding tensor for this nucleus, two other components have negligible changes in values from the monomer to the target molecule.

The availability of ^{13}C solid-state NMR experimental data on anhydrous chitosan allows for additional examination of the accuracy of our calculated data.[16] As mentioned earlier, unlike the EFG calculation, quantum mechanical calculation of NMR properties yields just the absolute chemical shielding tensors where eq 5 can be used for comparing them with the experimental values. However, the calculated ^{13}C chemical shielding values were referred to TMS, σ_{iso} = 184.1 ppm.[54] As the results in the Figure 2 indicate, there is a significant correlation between the calculated ^{13}C isotropic chemical shifts of target molecule and experimental values. Specifically, the slope of 0.990 and an R^2 value of 0.985 are approximately unity, which is an ideal acceptable index. Because the correlation coefficient can be taken as an index to characterize the quality of the calculated results, such a good agreement indicates that the H-bonding and other electrostatic effects encountered in the anhydrous chitosan cluster are sufficiently described when the neighboring chains are represented only by monomer units.

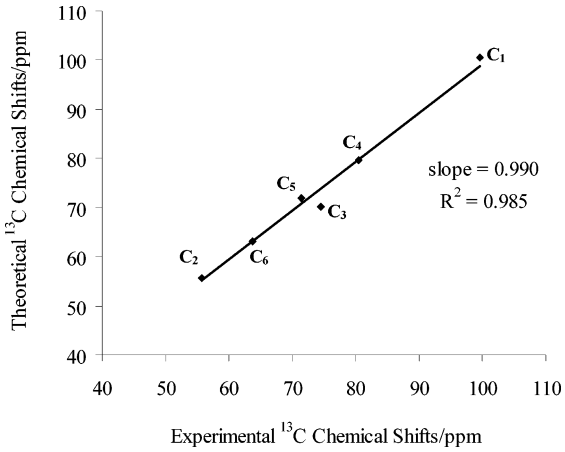

Figure 2. Comparison between the experimental and calculated (B3LYP/6-311++G(d,p)) ^{13}C chemical shifts for anhydrous chitosan. All experimental ^{13}C chemical shifts are from ref 16. Calculated isotropic chemical shielding values were referred to absolute isotropic value of TMS ($\sigma_{iso,ref}$ = 184.1 ppm).

4.3. Orientation of EFG and Chemical Shielding Tensors in Molecular Frame Axes. High level quantum chemical calculations have proven to be an excellent approach for obtaining EFG and chemical shielding tensor orientations. In general, the EFG and chemical shielding tensors have different orientations in the molecular frame of reference. Therefore, we must consider the relative orientation between the two tensors using three Euler angles (α, β, γ). Recently, Wu et al. have indicated that quantum chemical calculation at the B3LYP/6-311++G(d,p) level can produce reliable results for chemical shielding and EFG tensor orientations, although the magnitude of individual principal components computed by this level is less accurate.[64] Therefore, at this point, it is of much interest to characterize the relative orientation of the principal components of EFG and chemical shielding tensors in the anhydrous chitosan molecular frame. To fulfill this aim, calculated EFG and chemical shielding tensors of oxygen and nitrogen were analyzed systematically to obtain their eigenvectors. Following the approach of Eichele et al.,[65] three Euler angles were calculated and tabulated in Table 7.

As seen from Figure 3, it is indicated that σ_{33} and q_{xx} of the O(3) atom have a tendency to orientate along its none-bonding electron pair whereas the σ_{11} and q_{zz} components are along the O(3)···O(6−3) hydrogen bond direction. More specifically, σ_{33} and q_{zz} components make 54.50° and 25.57° angles with nonbonding pair and O(3)···O(6−3) hydrogen bond direction, respectively. Such orientations are in good agreement with the results obtained for other functional groups containing O−H bond such as carboxylic acids and alcohols.[20,66,67] However, at the O(5) site, the EFG and chemical shielding tensor orientations have opposite trends: σ_{11} and σ_{33} are approximately in the plane of the H(33)···O(5) hydrogen bond plane, but σ_{22} orientates along the norm of this plane. The smallest shielded component makes a 54.70° tilt angle with the O(5)···H(33) hydrogen bond, but the smallest component of the EFG tensor is tilted 39.60° from this hydrogen bond. For the O(6) atom, the relative orientation of EFG and chemical shielding tensors is slightly different. In this case, σ_{11} is almost perpendicular to the O(6)−H(63) bond and the q_{xx} component is away from this bond by 124.4°. Also, according to the findings in Figure 3, the orientation of the EFG tensor components at the nitrogen site is obtained so that the q_{zz} component makes a 7.98° angle with the nitrogen nonbonding pair direction and q_{yy} lies in the N−C(3) bond orientation. In addition, for the chemical shielding

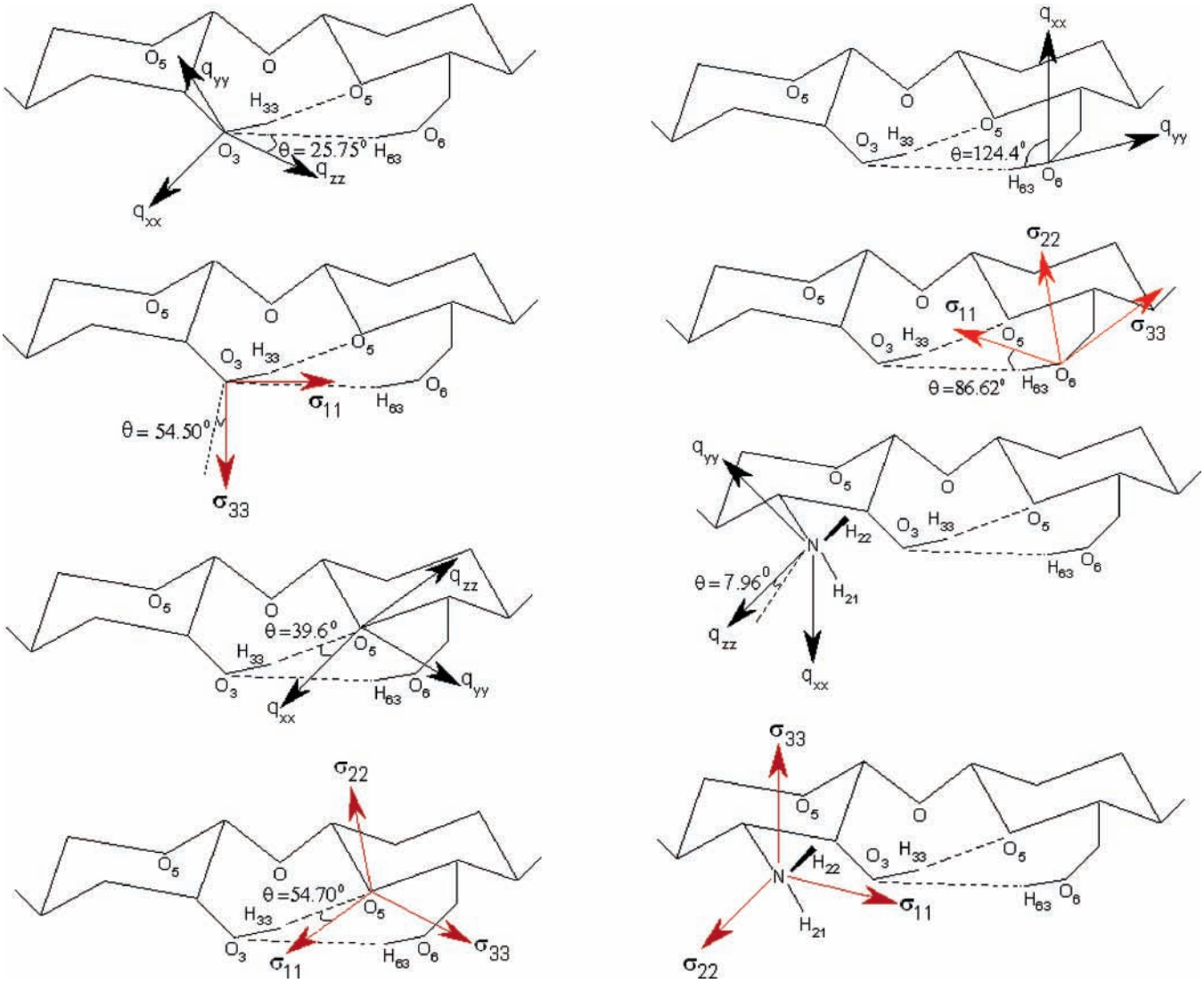

Figure 3. Illustration of orientations of the EFG and chemical shielding tensors of oxygen and nitrogen atoms for anhydrous chitosan calculated with B3LYP/6-311++G(d,p) method.

tensor the unique component is σ_{22}, which orientates in the nonbonding pair direction, and σ_{11} is directed in the H(21)-N−H(22) plane.

5. Conclusion

On the basis of the results obtained in this investigation, it is concluded that both EFG and chemical shielding tensors of oxygen, nitrogen, and hydrogen atoms in the HBs are appropriate parameters to characterize the property of these interactions. The B3LYP method with the 6-311++G(d,p) and 6-31++G(d,p) standard basis sets were employed to obtain these parameters through considering a hexameric cluster. However, the isotropic chemical shielding value of the ^{15}N nucleus was determined to be 220.79 ppm. This nucleus belongs to the amine group of the target molecule. In addition, it is noteworthy that although we considered the central chain in the trimer and neighbor chains in monomer units within the hexameric cluster, the effect of H-bonding and other long-range interactions on the calculated parameters are clearly observed. The calculated ^{13}C chemical shifts for the target molecule agree well with experimental values. However, the obtained slope and R^2 value are close to ideal unity, which is good evidence of the reliability of the proposed molecular model and calculation methods. Finally, we calculated the relative orientations of EFG and chemical shielding at the B3LYP/6-311++G(d,p) level of theory for oxygen and nitrogen atoms. All calculated orientations match related similar cases. Specifically, for the ^{14}N EFG tensor, the greatest principal component makes a 7.96° angle with its nonbonding electron pair direction, whereas for the chemical shielding tensor, the central component lies in this direction.

References and Notes

(1) Aspinal, G. O. *The Polysaccharides*; Academic Press: Orlando, FL, 1983.
(2) Kanauchi, K.; Deuchi, K.; Imasta, Y.; Shizukuishi, M.; Kobayashi, E. *Biosci. Biotech. Biochem.* **1995**, *59* (5), 786.
(3) Maeda, Y.; Kimura, Y. *Nutr. Cancer* **2004**, *134* (4), 945.
(4) Vila, A.; Sánchez, A.; Janes, K.; Behrens, I.; Kissel, T.; Jato, J. L. V.; Alonso, M. J. *Euro. J. Pharm. Biopharm.* **2004**, *57*, 123.
(5) Bernkop-Schnürchö, A.; Kast, C. E. *Adv. Drug Deliv. Rev.* **2001**, *52*, 127.
(6) Kumar, M. N. V. R. *React. Funct. Polym.* **2000**, *46*, 1.
(7) Leworasirikul, A.; Yokyama, S.; Noguchi, K.; Ogawa, K.; Okuyama, K. *Carbohydr. Res.* **2004**, *339*, 825.
(8) Yui, T.; Imada, K.; Okuyama, K.; Obata, Y.; Suzuki, K.; Ogawa, K. *Macromolecules* **1994**, *27*, 7601.
(9) Ogawa, K.; Yui, T.; Okuyama, K. *Int. J. Biol. Macromol.* **2004**, *34*, 1.
(10) Siraleartmukul, K.; Siriwong, K.; Remsungnen, T.; Muangsin, N.; Udomkichdecha, W.; Hannongbua, S. *Chem. Phys. Lett.* **2004**, *395*, 233.
(11) Sack, I.; Macholl, S. *Appl. Magn. Reson.* **1999**, *17*, 413.
(12) Lee, D.-K.; Ramamoorthy, A. *J. Magn. Reson.* **1998**, *113*, 204.

(13) Liwang, A. C.; Bax, A. *J. Magn. Reson.* **1997**, *127*, 54.
(14) Gu, Z.; Ridenour, C. F. *J. Am. Chem. Soc.* **1996**, *118*, 822.
(15) Gerald, R., II; Bernhard, T.; Haeberlen, U.; Rendell, J.; Opella, S. *J. Am. Chem. Soc.* **1993**, *115*, 777.
(16) Saitô, H.; Tabeta, R.; Ogawa, K. *Macromolecules* **1987**, *20*, 2424.
(17) Heux, L.; Brugnerotto, j.; Desbrières, J.; Vessali, M.-F.; Rinaudo, M. *Biomacromolecules* **2000**, *1*, 746.
(18) Mehring, M. *Principles of High Resolution NMR in Solids*; Springer: Berlin, 1983.
(19) Yamada, K.; Dong, S.; Wu, G. *J. Am. Chem. Soc.* **2000**, *122*, 11602.
(20) Wong, A.; Kevin, K. J.; Jenkins, R.; Clarkson, G. J.; Anupõld, T.; Howes, A. P.; Crout, D. H. G.; Samoson, A.; Dupree, R.; Smith, M. E. *J. Phys. Chem. A* **2006**, *110*, 1824.
(21) Facelli, J. C. *Chem. Phys. Lett.* **2000**, *322*, 91.
(22) Ida, R.; Clerk, M. D.; Wu, G. *J. Phys. Chem. A* **2006**, *110* (3), 1065.
(23) Facelli, J. C.; Pugmire, R. J.; Grant, D. M. *J. Am. Chem. Soc.* **1996**, *118*, 5488.
(24) Wu, G.; Yamada, K.; Dong, S.; Gronday, H. *J. Am. Chem. Soc.* **2000**, *122*, 4215.
(25) Scheurer, C.; Skrynnikov, N. R.; Lienin, S. F.; Straus, S. K.; Brüschweier, R.; Ernst, R. R. *J. Am. Chem. Soc.* **1999**, *121*, 4242.
(26) Nogaj, B. *J. Phys. Chem.* **1987**, *91*, 5863.
(27) Hunt, M. J.; Mackay, A. L. *J. Magn. Reson.* **1976**, *22*, 295.
(28) Hunt, M. J.; Mackay, A. L. *J. Magn. Reson.* **1974**, *152*, 402.
(29) Das, T. P.; Han, E. L. *Nuclear Quadrupole Resonance Spectroscopy*; Academic Press: New York, 1958.
(30) Bersohn, R. *J. Chem. Phys.* **1952**, *20* (10), 1505.
(31) Yu, G.; Morin, F. G.; Nobes, G. A. R.; Marchessault, R. H. *Macromolecules* **1999**, *32*, 518.
(32) Rappé, A. K.; Bernstein, E. R. *J. Phys. Chem. A* **2000**, *104*, 6117.
(33) Sim, F.; St-Amant, A.; Papai, I.; Salahub, D. R. *J. Am. Chem. Soc.* **1992**, *114*, 4391.
(34) Hamman, D. R. *Phys. Rev. B* **1997**, *55*, 10157.
(35) Xantheas, S. S. *J. Chem. Phys.* **1995**, *102*, 4505.
(36) Ireta, J.; Neugebauer, J.; Scheffler, M. *J. Phys. Chem. A* **2004**, *108*, 5692.
(37) Van Gisbergen, S. J. A.; Snijders, J. G.; Baerends, E. J. *J. Chem. Phys.* **1995**, *103*, 9347−9354.
(38) Salek, P.; Vahtras, O.; Helgaker, T.; Agren, H. *J. Chem. Phys.* **2002**, *117*, 9630.
(39) Helgaker, H.; Wilson, P. J.; Amos, R. D.; Handy, N. C. *J. Chem. Phys.* **2000**, *113*, 2088.
(40) Cheeseman, J. R.; Frisch, M. J.; Stephens, F. J.; Stephens, P. J. *J. Phys. Chem. A* **2000**, *104*, 1039.
(41) Ruud, K.; Helgaker, T. *Chem. Phys. Lett.* **2002**, *352*, 533.
(42) Cappeli, C.; Mennucci, B.; Tomasi, J.; Cammi, R.; Rizzo, A. *Chem. Phys. Lett.* **2001**, *346*, 251.
(43) Elmi, F.; Hadipour, N. L. *J. Phys. Chem. A* **2005**, *109*, 1729.
(44) Mirzaei, M.; Hadipour, N. L. *J. Phys. Chem. A* **2006**, *110*, 4833.
(45) Dong, S.; Ida, R.; Wu, G. *J. Phys. Chem. A* **2000**, *104*, 11194.
(46) Duer, M. J. Solid State NMR Spectroscopy; Blackwell Science Ltd.: London, 2002.
(47) Lucken, E. A. C. *Nuclear Quadrupole Coupling Constants*; Academic Press: London, 1992.
(48) Frisch, M. J.; Trucks, G. W.; Schlegel, H. B.; Scuseria, G. E.; Robb, M. A.; Cheeseman, J. R.; Zakrzewski, V. G.; Montgomery, J. A.; Stratmann, R. E.; Burant, J. C.; Dapprich, S.; Millam, J. M.; Daniels, A. D.; Kudin, K. N.; Strain, M. C.; Farkas, O.; Tomasi, J.; Barone, V.; Cossi, M.; Cammi, R.; Mennucci, B.; Pomelli, C.; Adamo, C.; Clifford, S.; Ochterski, J.; Petersson, G. A.; Ayala, P. Y.; Cui, Q.; Morokuma, K.; Malick, D. K.; Rabuck, A. D.; Raghavachari, K.; Foresman, J. B.; Cioslowski, J.; Ortiz, J. V.; Stefanov, B. B.; Liu, G.; Liashenko, A.; Piskorz, P.; Komaromi, I.; Gomperts, R.; Martin, R. L.; Fox, D. J.; Keith, T.; Al-Laham, M. A.; Peng, C. Y.; Nanayakkara, A.; Gonzalez, C.; Challacombe, M.; Gill, P. M. W.; Johnson, B.; Chen, W.; Wong, M. W.; Andres, J. L.; Head-Gordon, M.; Replogle, E. S.; Pople, J. A. *Gaussian 98*, revision A.6; Gaussian, Inc.: Pittsburgh, PA, 1998.
(49) Clark, T.; Chandrasekhar, J.; Spitznagel, G. W.; Schleyer, P. v. R. *J. Comp. Chem.* **1983**, *4*, 294.
(50) Behzadi, H.; Hadipour, N. L.; Mirzaei, M. *Biophys. Chem.* **2007**, *125*, 179.
(51) Waddell, K. W., Chekmenev, E. Y.; Wittebort, R. J. *J. Phys. Chem. B* **2006**, *110* (45), 22935.
(52) Mazeau, K.; Winter, W.; Chanzy, H. *Macromolecules* **1994**, *27* (26), 7606.
(53) Wolinski, K.; Hilton, J. F.; Pulay, P. *J. Am. Chem. Soc.* **1990**, *112*, 8251.
(54) Jameson, A. K.; Jameson, C. *J. Chem. Phys. Lett.* **1987**, *134*, 461.
(55) Anderson-Altmann, K. L.; Phung, C. G.; Mavromoustakos, S.; Zheng, Z.; Facelli, J. C.; Poulter, C. D.; Grant, D. M. *J. Phys. Chem.* **1995**, *99*, 10454.
(56) Pyykkö, P. *Mol. Phys.* **2001**, *99* (19), 1617.
(57) Boys, S. F.; Bernardi, F. *Mol. Phys.* **1970**, *19*, 553.
(58) Le, H.; Oldfield, E. *J. Phys. Chem.* **1996**, *100*, 16423.
(59) Pecul, M.; Sadlej, J. *Chem. Phys.* **1999**, *248*, 27.
(60) Mirzaei, M.; Elmi, F.; Hadipour, N. L. *J. Phys. Chem B* **2006**, *110*, 10991.
(61) Chesnut, D. B.; Rusiloski, B. E. *J. Phys. Chem.* **1993**, *97*, 2839.
(62) Strohmeier, M.; Stueber, D.; Grant, D. M. *J. Phys. Chem. A* **2003**, *107*, 7629.
(63) Tuttle, T.; Grä1fenstein, J.; Wu, A.; Kraka, E.; Cremer D. *J. Phys. Chem. B* **2004**, *108*, 1115.
(64) Wu, G.; Dong, S.; Ida, R.; Reen, N. *J. Am. Chem. Soc.* **2002**, *124* (8), 1768.
(65) Eichele, K.; Wasylishen, R. E.; Nelson, J. H. *J. Phys. Chem. A* **1997**, *101*, 5463.
(66) Bulter, G.; Brown, T. L. *J. Am. Chem. Soc.* **1981**, *103* (22), 6541.
(67) Gready, J. E. *J. Phys. Chem.* **1984**, *88*, 3497.